S. T. AKKOYUN

ÇANKAYA UNIVERSITY

RADIUS OF CURVATURE OF BESSEL-GAUSSIAN BEAM

SIDIKA TÜRKAN AKKOYUN

SEPTEMBER, 2012

ÇANKAYA UNIVERSITY
GRADUATE SCHOOL OF NATURAL AND APPLIED SCIENCES
ELECTRONIC AND COMMUNICATION ENGINEERING

MASTER THESIS

RADIUS OF CURVATURE OF BESSEL-GAUSSIAN BEAM

SIDIKA TÜRKAN AKKOYUN

SEPTEMBER, 2012

Title of Thesis : **Radius of Curvature of Bessel-Gaussian Beam**

Submitted by : **Sıdıka Türkan AKKOYUN**

Approval of the Graduate School of Natural and Applied Sciences, Çankaya University

----

Prof. Dr. Taner ALTUNOK
Director

I certify that this thesis satisfies all the requirements as a thesis for the degree of Master of Science.

Prof. Dr. Celal Zaim ÇİL
Head of Department

This is to certify that we have read this thesis and that in our opinion it is fully adequate, in scope and quality, as a thesis for the degree of Master of Science.

Prof. Dr. Yusuf Ziya UMUL
Supervisor

Examination Date: 11.09.2012

Examining Committee Members:

Assist. Prof. Dr. Barbaros PREVEZE	(Çankaya University)	....
Prof. Dr. Yusuf Ziya UMUL	(Çankaya University)	....
Research Assist. Filiz SARI	(Ankara University)	....

STATEMENT OF NON PLAGIARISM

I hereby declare that all information in this document has been obtained and presented in accordance with academic rules and ethical conduct. I also declare that, as required by these rules and conduct, I have fully cited and referenced all material and results that are not original to this work.

Name, Last Name: SIDIKA TÜRKAN AKKOYUN

Signature :

Date : 13.06.2013

ABSTRACT

RADIUS OF CURVATURE OF BESSEL-GAUSSIAN BEAM

AKKOYUN, Sıdıka Türkan

M.Sc., Department of Electronic and Communication Engineering

Supervisor: Prof. Dr. Yusuf Z. UMUL

September 2012, 28 pages

In this thesis, for a turbulent atmosphere, the radius of curvature of Bessel-Gaussian beam is formulated. For various order of Bessel-Gaussian beam of the first kind, the source size, propagation distance, wavelength, this formula is analyzed numerically in moderate turbulence, high turbulence and under free space condition. Results have shown that Bessel-Gaussian beam behaves as Gaussian beam and radius of curvature of Bessel-Gaussian beam decreases with growing turbulence levels. Results have also shown that the radius of curvature increases with the increasing source size and changes slowly with the wavelength.

Keywords: Bessel Gaussian beam, radius of curvature, Gaussian beam, intensity, Gaussian beam width

ÖZET

BESSEL-GAUSSIAN IŞIK DEMETİNİN EĞRİLİK YARIÇAPI

AKKOYUN, Sıdıka Türkan

Yüksek Lisans, Elektronik ve Haberleşme Mühendisliği Bölümü

Yönetici: Prof. Dr. Yusuf Z. UMUL

Eylül 2012, 28 sayfa

Tezde, türbülanslı atmosfer ortamında Bessel-Gaussian ışık demetinin eğrilik yarıçapını veren bir eşitlik önerilmiş ve Bessel-Gaussian ışık demetinin eğrilik yarıçapı, Bessel fonksiyonunun ilk türünün farklı dereceleri, kaynak boyutları, hüzmenin yayılma mesafesi ve dalga boyları için ortalama türbülans, yüksek türbülans ve türbülansın olmadığı seviyelerde analiz edilmiştir. Sonuçlar Bessel-Gaussian ışık demetinin Gaussian ışık demeti gibi davrandığını ve Bessel-Gaussian ışık demetinin eğrilik yarıçapının artan türbülans seviyeleriyle azaldığını göstermiştir. Sonuçlar aynı zamanda eğrilik yarıçapının artan kaynak genişliği ile beraber arttığını ve dalga boyuyla yavaşça değiştiğini de göstermiştir.

Anahtar Kelimeler: Bessel Gaussian ışık demeti, eğrilik yarıçapı, Gaussian ışık demeti, ışık şiddeti, ışık demeti genişliği

ACKNOWLEDGMENTS

I present my best regards to my supervisor Prof. Dr. Yusuf Z. UMUL for his valuable assistance and contributions during my studies.

TABLE OF CONTENTS

LIST OF TABLES

LIST OF FIGURES

LIST OF SYMBOLS AND ABBREVIATIONS

α	:	Parameter Which Is Related to the Gaussian Source Size
α_s	:	Gaussian Source Size
$\alpha_r^2(z)$	:	Radial Second Moment
$\alpha_{r\phi}^2(z)$	:	Radial-Angular Second Moment
$\alpha_\phi^2(z)$	:	Angular Second Moment
$\alpha_{fsr}^2(z)$	:	Radial Second Moment at Free Space
θ	:	Beam Divergence
κ	:	Spatial Frequency
λ	:	Wavelength
Φ	:	Gaussian Phase
$\phi_n(\kappa)$	:	Spectrum Function
$\omega(z)$	:	Beam Width
a_B	:	Width Parameter
C_n^2	:	Structure Constant
F_0	:	Gaussian Focusing Parameter
FSO	:	Free Space Optic
H	:	Integration over Spatial Frequencies of the Spectrum Function
$I_r(r,z)$	:	Receiver Intensity
$I_{fsr}(r)$	:	Receiver Intensity at Free Space
$I_n(x)$	:	Modified Bessel Function
j	:	Imaginary Number
J_n	:	Bessel Function of the First Kind
k	:	Wave Number
l_0	:	Inner Scale of Turbulence

L_0	:	Outer Scale of Turbulence
n	:	Order of the Bessel Function of the First Kind
$R(z)$	:	Radius of Curvature
$U(r, z)$	:	Gaussian Field Distribution at Receiver
$U_s(r, \phi_s)$	:	Bessel-Gaussian Field Distribution at Source
$U_r(r, \phi_r)$	:	Bessel-Gaussian Field Distribution at Receiver
$Y_n(x)$	:	Bessel Function of Second Kind
*	:	Complex Conjugate

INTRODUCTION

Free space optical communication (FSO) systems operate in the infrared spectrum [1] and use free space (atmosphere) as transmitting media, in other words signal is transmitted between receiver and transmitter without cables in these systems. FSO has been came forward in recent years, since FSO supplies broadband, high speed data transfer, lower costs and no interference [2]. Against these advantages, there are disadvantages from atmospheric effects, i.e. fog, rain, solar warming, absorption from atmospheric gases [3]. In FSO communication, LEDs and lasers are usually used. So, propagation and properties of laser beam have been important.

Lasers have optical resonator where amplified, monochromatic, inphase, linear beam is obtained. This beam propagation usually approximates Gaussian intensity profile. In this context, Gaussian beam propagation and its optical properties have been studied often to improve laser communication. Different optical properties of Gaussian beam have been researched under different conditions. Radius of curvature is also optical property of the laser beams which is major factor for laser beam shaping. In the previous studies, the effects of atmospheric turbulence have been researched on the radius of curvature for hyperbolic, sinusoidal, annular, dark hollow and flat topped Gaussian beams [4, 5].

The purposes of this study are to obtain radius of curvature of Bessel-Gaussian beam analytically, examine effects of different turbulence levels on radius of curvature of Bessel-Gaussian beam numerically, show that Bessel-Gaussian beam follow trend of Gaussian beam, compare Bessel-Gaussian beam and Gaussian beam.

In Chapter I, Gaussian beam and its properties are mentioned for understanding how a beam, which has a Gaussian beam profile, should behave. It is mentioned beam parameters of a Gaussian beam such as, field, intensity, power, beam width, beam divergence, depth of focus, phase and radius of curvature. By this way, the general information is presented about behavior of Gaussian beams. Radius of curvature of a Gaussian beam is also plotted in free space by the help of MATLAB. Bessel-Gaussian beam and Bessel functions are mentioned briefly.

In the first part of Chapter II, Radius of curvature of the Bessel-Gaussian beam is derived analytically using the previous study. In the second part of Chapter II, accuracy of the formula for the radius of curvature of Bessel-Gaussian beam is verified under stated conditions and is commented with the help of MATLAB. In the last part of Chapter II, radius of curvature of the Bessel-Gaussian beam is obtained numerically and graphics is plotted. The Bessel-Gaussian and the Gaussian beams are compared. It is shown that the Bessel-Gaussian beam acts similar as a Gaussian beam.

CHAPTER I

BESSEL-GAUSSIAN BEAM

1.1. GAUSSIAN BEAM AND BEAM PARAMETERS

Gaussian beam is defined as electromagnetic beam by function of Gaussian with electrical field and intensity. Its mathematical function is a solution of paraxial Helmholtz equation. Field of Gaussian beam is given in [6] as;

$$U_r(r,z) = U_0 \frac{\alpha_s}{\omega(z)} \exp\left(-\frac{r^2}{\omega(z)^2}\right) \exp\left[-j\left(kz - \tan^{-1}\frac{z}{z_R}\right) - j\frac{kr^2}{2R(z)}\right], \tag{1.1}$$

where r is radial distance, z is axial distance(propagation distance), $k = 2\pi/\lambda$ is wave number, λ is wavelength, E_0 is the field at the center, z_R is the Rayleigh range which is defined by $\pi\alpha_s^2/\lambda$, $R(z)$ is radius of curvature, α_s is source size and $\omega(z)$ is beam width.

Source size α_s and beam width $\omega(z)$ are beam parameters. They are shown below respectively, which are taken from [7].

$$\alpha_s = \sqrt{\frac{\lambda z_R}{\pi}}. \tag{1.2}$$

$$\omega(z) = \alpha_s \sqrt{\left(1 + \left(\frac{z}{z_R}\right)^2\right)}. \tag{1.3}$$

Expanse of Gaussian beam is beam width along z propagation direction. Figure 1.1 is plotted by using equation (1.3) and includes $-\omega(z)$ for easy to understand beam parameters. From Figure 1.1 it is clear that the beam width is at its minimum value at $z = 0$, which is known as beam waist or source size, after that beam expands, i.e. the beam width increases. On the other hand spot size is equal to $2\alpha_s$.

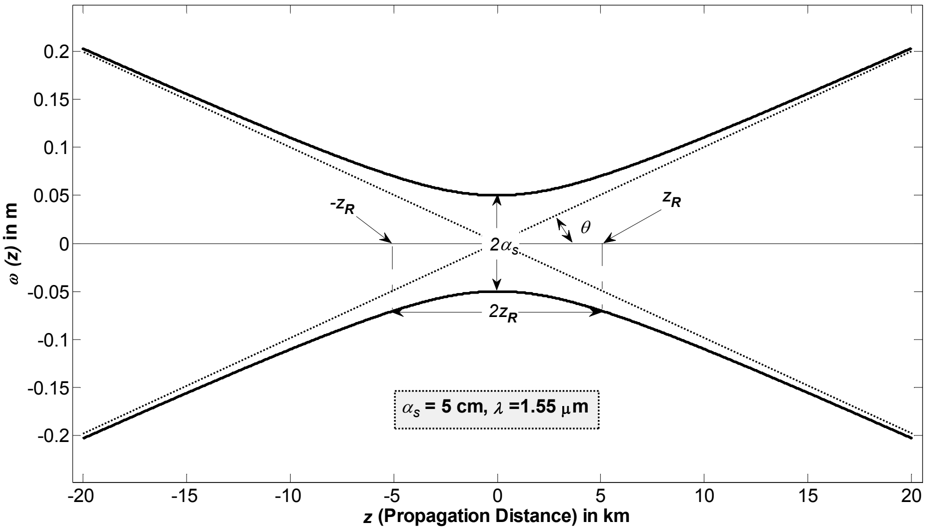

Figure 1.1 Variations of beam width of Gaussian beam versus propagation distance at fixed source size and wavelength

In Figure 1.1, θ is the beam divergence, which is another beam parameter. θ is the angle with z axis of wavefront of the Gaussian beam and can be written by using paraxial approach as;

$$\tan(\theta) \approx \theta = \frac{\alpha_s}{z_R}. \tag{1.4}$$

When Rayleigh range is substituted into equation (1.4), beam divergence is

$$\theta = \frac{\lambda}{\pi\alpha_s}. \tag{1.5}$$

From equation (1.5), it is clear that highly directed beam can be obtained by using short wavelength and thick waist. In other words, if the beam divergence decreases, the beam will becomes more directed.

Depth of focus is also a beam parameter, which is defined as $2z_R$ long. This parameter is shown in Figure 1.1 and is expressed by

$$2z_R = \frac{2\pi\alpha_s^2}{\lambda}. \tag{1.6}$$

From equation (1.6), it is seen that the depth focus is inversely proportional with wavelength and directly proportional with the area of spot size (i.e. $\pi\alpha_s^2$). In this area, Gaussian beam achieves best focus.

From (1.1), the phase of Gaussian beam is

$$\varphi = kz - \tan^{-1}\frac{z}{z_R} + \frac{kr^2}{2R(z)}. \tag{1.7}$$

The phase is on the beam axis

$$\varphi = kz - \tan^{-1}\frac{z}{z_R}, \tag{1.8}$$

where kz is the phase of plane wave and $\tan^{-1}(z/z_R)$ is the phase retardation, which causes delay of the wavefront. From $z = -\infty$ to $z = \infty$, total phase retardation is π, which is the Gouy effect.

1.2. INTENSITY OF THE GAUSSIAN BEAM

The intensity of the Gaussian beam is calculated by the power per unit area [7] and it is equal to the square of its complex field, which is given in [7] as;

$$I_r(r,z) = |U(r,z)|^2. \tag{1.9}$$

If equation (1.1) is substituted into equation (1.9), intensity of Gaussian beam would be

$$I_r(r,z) = I_0\left[\frac{\alpha_s}{\omega(z)}\right]^2 \exp\left[-\frac{2r^2}{\omega(z)^2}\right], \tag{1.10}$$

where I_0 is the intensity at the source. Unit of $I_r(r,z)$ is watts/m^2. Figure 1.2 is plotted by using equation (1.10) at $r = 0$. From Figure 1.2, it is clear that normalized intensity of Gaussian beam reaches its maximum value at $z = 0$. At $z = z_R$, the intensity reaches $I_0/2$, namely it has half of maximum value . At larger z, the intensity decreases.

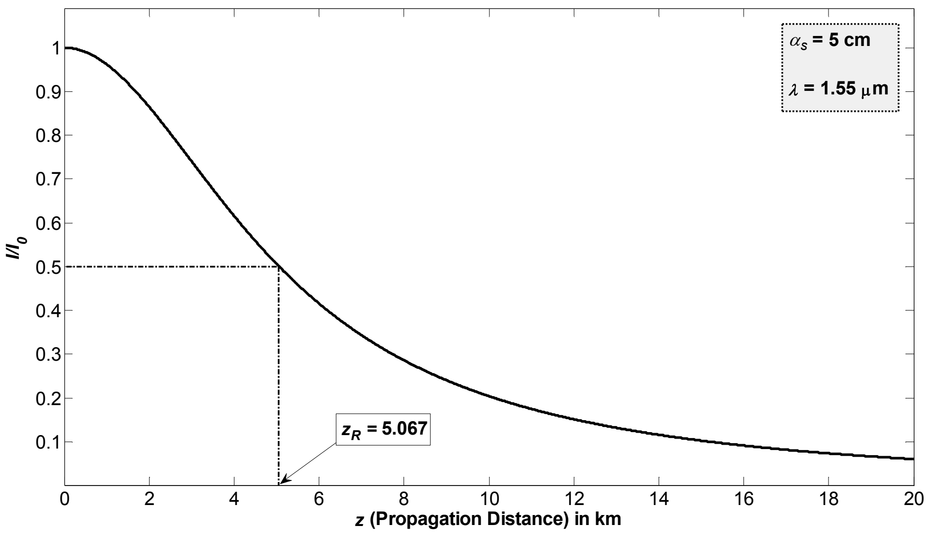

Figure 1.2 Variations of normalized intensity of the Gaussian beam versus propagation distance at fixed source size and wavelength

The optical power P, which is carried by Gaussian beam, is integral of intensity of Gaussian beam. The optical power is given in [7] as;

$$P = \int_0^\infty I_r(r,z) 2\pi dr. \tag{1.11}$$

1.3.RADIUS OF CURVATURE OF THE GAUSSIAN BEAM

In general, the radius of curvature is a parameter, which is inversely proportional to curvature of surfaces. If the radius of curvature increases, surfaces will become more flat. For example, the radius of earth is $6{,}371$ km and the earth appears to us as if it is flat. Similarly, for a beam, if the radius of curvature of wavefront deacreses, the wavefront is more flat.

In equation (1.7), term of $kr^2/2R(z)$ causes to curvature of wavefront. This situation is shown in Figure (1.3). The radius of curvature of the Gaussian beam can be given in [7] as;

$$R(z) = z\left[1 + \left(\frac{z_R}{z}\right)^2\right]. \tag{1.12}$$

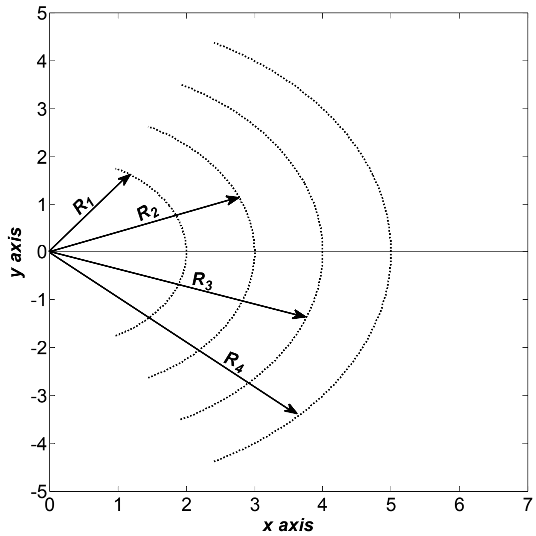

Figure 1.3 Bending of wavefronts with increasing radius of curvature

If the Rayleigh range (z_R) is substituted into equation (1.12), the radius of curvature will become

$$R(z) = z\left[1 + \left(\frac{\pi\alpha_s^2}{z\lambda}\right)^2\right]. \tag{1.13}$$

After some simplifications, the radius of curvature can be written as

$$R(z) = 0.25z^{-1}(k^2\alpha_s^4 + 4z^2). \tag{1.14}$$

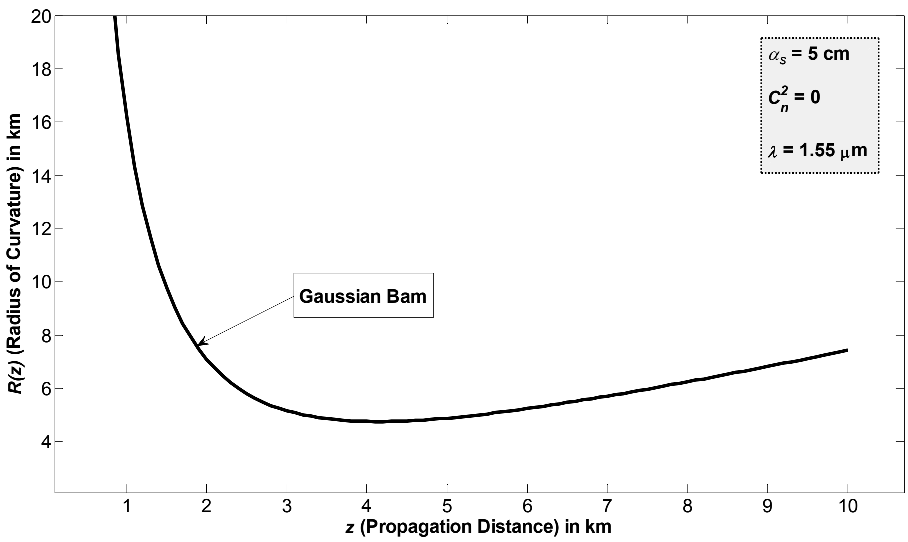

Figure 1.4 Variations of radius of curvature versus propagation distance under free space conditions at fixed source size and wavelength

Figure 1.4 is obtained by using equation (1.14). Figure 1.4 shows that the radius of curvature is infinite at first, namely there is no wavefront bending and the radius of curvature reaches minimum value at $z = z_R$. After that point, the radius of curvature increases with increasing z.

1.4. THE BESSEL FUNCTIONS

The Bessel differential equation is obtained by using cylindrical coordinates for three dimensional Laplace in Cartesian coordinate, which is given in [8] as;

$$x^2y'' + xy' + (x^2 - n^2)y = 0 \tag{1.14}$$

where n is known as order argument and constant. Functions, which are solutions of equation (1.14), are called n-th order Bessel functions. In Bessel differential equation, since point of $x = 0$ is singular, solution of (1.14) is obtained by using Frobenius method. For solution, this method uses series as;

$$y = x^p \sum_{k=0}^{\infty} a_k x^k. \tag{1.15}$$

If n is a non-integer, equation (1.14) has two solutions as J_{-n} and J_n, which are called the Bessel functions of the first kind . Figure 1.5 represents the Bessel function of the first kind, which is plotted by using MATLAB. These functions are given in [8] as;

$$J_n(x) = \sum_{k=0}^{\infty} \frac{(-1)^k}{k!\,\Gamma(n+k+1)} \left(\frac{x}{2}\right)^{n+2k}, \tag{1.16}$$

where $J_{-n}(x)$ can be obtained by replacing n with $-n$ and $I_n(x)$, which is the modified Bessel function, can be obtained by replacing x with xi. So, general solution of the Bessel differential equation can be written as;

$$y(x) = c_1 J_n(x) + c_2 J_{-n}(x), \tag{1.17}$$

where c_1 and c_2 are arbitrary constants.

If n is a non-integer, general solution of the Bessel differential equation cannot be written as equation (1.17). Hence, a function is defined as;

$$Y_n(x) = \frac{J_n(x)\cos(n\pi) - J_{-n}(x)}{\sin(n\pi)} \tag{1.18}$$

which is called the Bessel function of the second kind and also known as The Neumann or The Weber function. As a result, for all valid of n, a general solution can be written as;

$$y(x) = c_1 J_n(x) + c_2 Y_n(x). \tag{1.19}$$

where c_1 and c_2 are arbitrary constants.

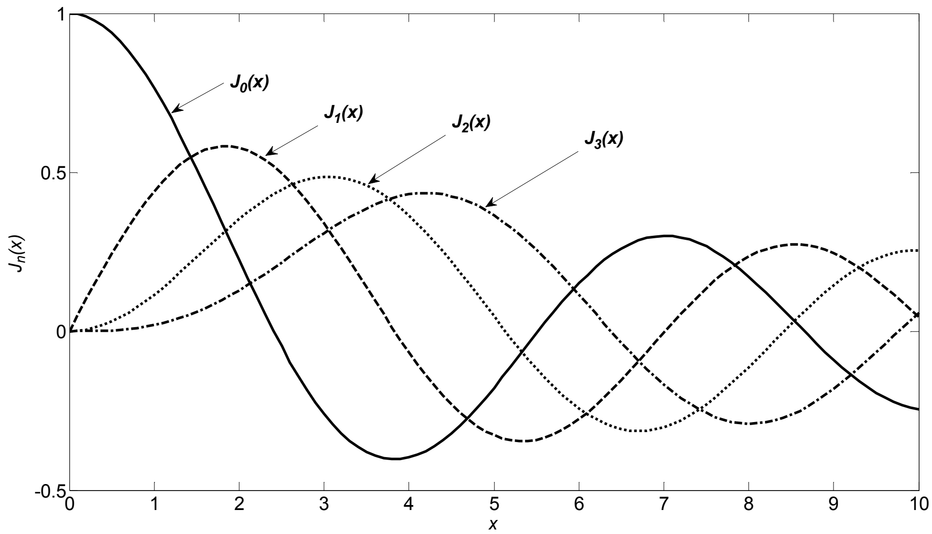

Figure 1.5 Bessel function of the first kind against x-axis for different order (n)

1.5. THE BESSEL-GAUSSIAN BEAM

The Bessel-Gaussian beam follows trend of the Gaussian beam and its field equation includes Bessel function. On the source plane, its field distribution is given in (3) of [9] as;

$$U_s(s, \phi_s) = \exp(-k\alpha s^2)\exp(-jn\phi_s)J_n(a_B s), \tag{1.20}$$

where s and ϕ_s are radial coordinates on a source plane, $k = 2\pi/\lambda$ is wavenumber, λ is wavelength, $\alpha = 1/(k\alpha_s^2) + j/(2F_0)$ is related to Gaussian beam source size α_s and focusing parameter F_0, s is radial distance, j is $\sqrt{-1}$, a_B defines the beam width and $n > 0$ is order of the Bessel function of the first kind $J_n(a_B s)$.

When the Bessel-Gaussian beam propagates at distance z from the source plane, the field is given in (4) of [9] as;

$$U_r(r,\phi_r) = -\frac{\exp(jkz)}{1+2j\alpha z}\exp(-jn\phi_r)\exp\left(-\frac{ja_B^2 z + 2\alpha k^2 r^2}{2k(1+2j\alpha z)}\right) \times J_n\left(\frac{a_B r}{1+2j\alpha z}\right) \tag{1.21}$$

where r and ϕ_r are radial coordinates on a receiver plane.

CHAPTER II

RADIUS OF CURVATURE BESSEL GAUSSIAN BEAM

2.1. DEVELOPMENT OF FORMULATION

From (3) of [10], at a distance of z from the source plane on a receiver plane, the radius of curvature is;

$$R(z) = \frac{\alpha_r^2(z)}{\alpha_{r\phi}^2(z)}, \tag{2.1}$$

where $\alpha_r^2(z)$ and $\alpha_{r\phi}^2(z)$ are respectively radial and radial-angular second moments. From (4a) and (4b) of [10], the numerator and the denominator of (2.1) are;

$$\alpha_r^2(z) = \alpha_r^2(0) + 2\alpha_{r\phi}^2(0)z + \alpha_\phi^2(0)z^2 + \frac{4\pi^2}{3}Hz^3, \tag{2.2a}$$

$$\alpha_{r\phi}^2(z) = \alpha_{r\phi}^2(0) + \alpha_\phi^2(0)z + 2\pi^2Hz^2, \tag{2.2b}$$

where at source plane, $\alpha_r^2(0)$, $\alpha_{r\phi}^2(0)$ and $\alpha_\phi^2(0)$ are respectively radial, radial-angular and angular second moments. H represents an integration over the spatial frequencies of the spectrum function $\phi_n(\kappa)$ and is given in (5) of [5] as;

$$H = \int_0^\infty \kappa^3\phi_n(\kappa)d\kappa, \tag{2.3}$$

where κ is the scalar spatial frequency. For $\phi_n(\kappa)$, modified von Karman spectrum is applied in developing formulation, which includes inner and outer scale parameters. So $\phi_n(\kappa)$ is given in [11] as;

$$\phi_n(\kappa) = \frac{0{,}033C_n^2 exp\left[-\left(\frac{l_0}{5{,}92}\right)^2\kappa^2\right]}{\left[\kappa^2 + \left(\frac{2\pi}{L_0}\right)^2\right]^{11/6}}, \tag{2.4}$$

where C_n^2 is a measure of strength of the fluctuations in the refractive index and is known as structure constant. Also, l_0 and L_0 are respectively inner and outer scales. So, expression (2.3) can be written with expression (2.4) and condition of $L_0 \to \infty$

$$H = 0{,}033 C_n^2 \int_0^\infty \kappa^{-2/3} exp\left[-\left(\frac{l_0}{5{,}92}\right)^2 \kappa^2\right] d\kappa. \tag{2.5}$$

As a result, H becomes (2.6) by use of Eq. (3.478.1) of [10].

$$H = 0.1661 \frac{C_n^2}{l_0^{1/3}}. \tag{2.6}$$

For calculation of the radius of curvature, it is necessary to obtain $\alpha_{fsr}^2(z)$, which is free space equivalence of $\alpha_r^2(L)$. From (6) of [5]

$$\alpha_r^2(z) = \alpha_{fsr}^2(z) + \frac{4\pi^2}{3} H z^3. \tag{2.7}$$

At a distance of z from the source plane on a receiver plane, $\alpha_{fsr}^2(z)$ can be adapted from (7) of [4], which is;

$$\alpha_{fsr}^2(z) = \frac{\int_0^\infty r^3 I_{fsr}(r) dr}{\int_0^\infty r I_{fsr}(r) dr}. \tag{2.8}$$

In equation (2.8), $I_{fsr}(r)$ is the free space receiver intensity of the Bessel-Gaussian Beam and given in (6) of [12] as;

$$\begin{aligned} I_{fsr}(r) = {} & \frac{b^2}{(k\alpha - jb)(k\alpha^* + jb)} exp\left[-\frac{a_B^2 + 4b^2 r^2}{2\alpha_s^2 (k\alpha - jb)(k\alpha^* + jb)}\right] \\ & \times J_n\left(\frac{j a_B r}{k\alpha - jb}\right) J_n\left(\frac{-j a_B r}{k\alpha^* + jb}\right), \end{aligned} \tag{2.9}$$

where r is radial distance, α_s is the Gaussian source size, $\alpha = 1/(k\alpha_s^2) + j/(2F_0)$ is related to the Gaussian source size, α^* is conjugate of α, $k = 2\pi/\lambda$ is wavenumber, b is $k/(2z)$ and j is $\sqrt{-1}$. If numerator and denominator of (2.8) are respectively called as A and B, numerator of (2.8) is;

$$A = \frac{b^2}{(k\alpha - jb)(k\alpha^* + jb)} exp\left[-\frac{a_B^2}{2\alpha_s^2(k\alpha - jb)(k\alpha^* + jb)}\right]$$
$$\times \int_0^\infty r exp\left[-\frac{4b^2r^2}{2\alpha_s^2(k\alpha - jb)(k\alpha^* + jb)}\right] \tag{2.10}$$
$$\times J_n\left(\frac{ja_Br}{k\alpha - jb}\right) J_n\left(\frac{-ja_Br}{k\alpha^* + jb}\right) dr.$$

And denominator of (2.8) is;

$$B = \frac{b^2}{(k\alpha - jb)(k\alpha^* + jb)} exp\left[-\frac{a_B^2}{2\alpha_s^2(k\alpha - jb)(k\alpha^* + jb)}\right]$$
$$\times \int_0^\infty r^3 exp\left[-\frac{4b^2r^2}{2\alpha_s^2(k\alpha - jb)(k\alpha^* + jb)}\right] \tag{2.11}$$
$$\times J_n\left(\frac{ja_Br}{k\alpha - jb}\right) J_n\left(\frac{-ja_Br}{k\alpha^* + jb}\right) dr.$$

For solution of (2.10), derivation of Eq. (6.633.2) of [10] with respect ρ is used, which is;

$$\int_0^\infty x^3 \exp(-\rho^2 x^2) J_p(\gamma x) J_p(\beta x) dx = \left[\left(\frac{1+p}{2\rho^4} - \frac{\gamma^2+\beta^2}{8\rho^6}\right) I_p\left(\frac{\gamma\beta}{2\rho^2}\right) + \frac{\gamma\beta}{4\rho^6} I_{p+1}\left(\frac{\gamma\beta}{2\rho^2}\right)\right] exp\left[-\frac{\gamma^2+\beta^2}{4\rho^2}\right]. \tag{2.12}$$

If equation (2.10) is adapted to equation (2.12), related parameters are

$$\rho^2 = \frac{4b^2}{2\alpha_s^2(k\alpha - jb)(k\alpha^* + jb)}, \tag{2.13a}$$

$$\gamma = j\frac{a_B b}{k\alpha - jb}, \tag{2.13b}$$

$$\beta = -j\frac{a_B b}{k\alpha^* + jb}, \tag{2.13c}$$

$$p = n, \tag{2.13d}$$

and numerator of (2.8) is;

$$
\begin{aligned}
A = {} & \frac{b^2}{(k\alpha - jb)(k\alpha^* + jb)} exp\left(-\frac{a_B^2}{2\alpha_s^2(k\alpha - jb)(k\alpha^* + jb)}\right) \\
& \times \left[\left(\frac{1+n}{2(4b^2)^2}\left(2\alpha_s^2(k\alpha - jb)(k\alpha^* + jb)\right)^2 \right.\right. \\
& - \frac{\left(-\frac{a_B^2 b^2}{(k\alpha - jb)^2} - \frac{a_B^2 b^2}{(k\alpha^* + jb)^2}\right)}{8(4b^2)^3} \\
& \left. \times \left(2\alpha_s^2(k\alpha - jb)(k\alpha^* + jb)\right)^3\right) I_n\left(\frac{a_B^2}{(k\alpha - jb)(k\alpha^* + jb)}\right) \\
& \left. + \frac{a_B^2 b^2\left(2\alpha_s^2(k\alpha - jb)(k\alpha^* + jb)\right)^3}{4(4b^2)^3(k\alpha - jb)(k\alpha^* + jb)} I_{n+1}\left(\frac{a_B^2}{(k\alpha - jb)(k\alpha^* + jb)}\right)\right] \\
& \times exp\left(-\frac{\left(-\frac{a_B^2 b^2}{(k\alpha - jb)^2} + \frac{a_B^2 b^2}{(k\alpha^* + jb)^2}\right) 2\alpha_s^2(k\alpha - jb)(k\alpha^* + jb)}{4(4b^2)}\right).
\end{aligned}
\tag{2.14}
$$

For solution of denominator of (2.8), Eq. (6.633.2) of [10] is used, which is

$$
\int_0^\infty x \exp(-\rho^2 x^2) J_p(\gamma x) J_p(\beta x) dx = \frac{1}{2\rho^2} exp\left[-\frac{\gamma^2 + \beta^2}{4\rho^2}\right] I_p\left(\frac{\gamma\beta}{2\rho^2}\right) \tag{2.15}
$$

And denominator of (2.8) is

$$
\begin{aligned}
B = {} & \frac{b^2}{(k\alpha - jb)(k\alpha^* + jb)} exp\left(-\frac{a_B^2}{2\alpha_s^2(k\alpha - jb)(k\alpha^* + jb)}\right) \\
& \times \frac{2\alpha_s^2(k\alpha - jb)(k\alpha^* + jb)}{2(4b^2)} I_n\left(\frac{a_B^2}{(k\alpha - jb)(k\alpha^* + jb)}\right) \\
& \times exp\left(-\frac{\left(-\frac{a_B^2 b^2}{(k\alpha - jb)^2} + \frac{a_B^2 b^2}{(k\alpha^* + jb)^2}\right) 2\alpha_s^2(k\alpha - jb)(k\alpha^* + jb)}{4(4b^2)}\right).
\end{aligned}
\tag{2.16}
$$

Finally, equation (2.8) becomes to

$$\alpha_{fsr}^2(z) = \frac{2(1+n)\alpha_s^2(k\alpha - jb)(k\alpha^* + jb)}{(4b^2)} + \frac{\alpha_B^2\alpha_s^4((k\alpha - jb)^2 + (k\alpha^* + jb)^2)}{4(4b^2)} + \frac{\alpha_B^2\alpha_s^4(k\alpha - jb)(k\alpha^* + jb)}{2(4b^2)} \frac{I_{n+1}\left(\frac{\alpha_B^2\alpha_s^2}{4}\right)}{I_n\left(\frac{\alpha_B^2\alpha_s^2}{4}\right)}. \tag{2.17a}$$

For using of $\alpha_{fsr}^2(z)$ in $\alpha_r^2(z)$, the coefficient of $\alpha_{fsr}^2(z)$ must be associated with the coefficient of $\alpha_r^2(z)$. $b = k/(2z)$ is used for associating equations and $j(\alpha - \alpha^*) = (-1/F_0)$ for the sake of simplicity, so $\alpha_{fsr}^2(z)$ is given by;

$$\alpha_{fsr}^2(z) = \frac{(1+n)\alpha_s^2}{2} + \frac{\alpha_B^2\alpha_s^4}{8}\left(\frac{I_{n+1}\left(\frac{\alpha_B^2\alpha_s^2}{4}\right)}{I_n\left(\frac{\alpha_B^2\alpha_s^2}{4}\right)} - 1\right) + 2z\left(-\frac{(1+n)\alpha_s^2}{2F_0} - \frac{\alpha_B^2\alpha_s^4}{8F_0}\left(\frac{I_{n+1}\left(\frac{\alpha_B^2\alpha_s^2}{4}\right)}{I_n\left(\frac{\alpha_B^2\alpha_s^2}{4}\right)} - 1\right)\right) + z^2\left(2(1+n)\alpha_s^2\alpha\alpha^* + \frac{\alpha_B^2\alpha_s^4\left(\alpha^2 + {\alpha^*}^2\right)}{4} + \frac{\alpha_B^2\alpha_s^4\alpha\alpha^*}{2} \times \left(\frac{I_{n+1}\left(\frac{\alpha_B^2\alpha_s^2}{4}\right)}{I_n\left(\frac{\alpha_B^2\alpha_s^2}{4}\right)}\right)\right). \tag{2.17b}$$

When $\alpha_{fsr}^2(z)$ is written in (2.7), $\alpha_r^2(z)$ is

$$\begin{aligned}\alpha_r^2(z) &= \frac{(1+n)\alpha_s^2}{2} + \frac{\alpha_B^2\alpha_s^4}{8}\left(\frac{I_{n+1}\left(\frac{\alpha_B^2\alpha_s^2}{4}\right)}{I_n\left(\frac{\alpha_B^2\alpha_s^2}{4}\right)} - 1\right) \\ &+ 2z\left(-\frac{(1+n)\alpha_s^2}{2F_0} - \frac{\alpha_B^2\alpha_s^4}{8F_0}\left(\frac{I_{n+1}\left(\frac{\alpha_B^2\alpha_s^2}{4}\right)}{I_n\left(\frac{\alpha_B^2\alpha_s^2}{4}\right)} - 1\right)\right) \\ &+ z^2\left(2(1+n)\alpha_s^2\alpha\alpha^* + \frac{\alpha_B^2\alpha_s^4\left(\alpha^2+{\alpha^*}^2\right)}{4} + \frac{\alpha_B^2\alpha_s^4\alpha\alpha^*}{2}\right. \\ &\left.\times\left(\frac{I_{n+1}\left(\frac{\alpha_B^2\alpha_s^2}{4}\right)}{I_n\left(\frac{\alpha_B^2\alpha_s^2}{4}\right)}\right)\right) + \frac{2.1857C_n^2z^3}{l_0^{1/3}}.\end{aligned} \tag{2.18}$$

By use of same coefficients between (2.2a) and (2.2b), $\alpha_{r\phi}^2(L)$ will become

$$\begin{aligned}\alpha_{r\phi}^2(z) &= -\frac{(1+n)\alpha_s^2}{2F_0} - \frac{\alpha_B^2\alpha_s^4}{8F_0}\left(\frac{I_{n+1}\left(\frac{\alpha_B^2\alpha_s^2}{4}\right)}{I_n\left(\frac{\alpha_B^2\alpha_s^2}{4}\right)} - 1\right) + z\left(2(1+n)\alpha_s^2\alpha\alpha^*\right. \\ &\left.+ \frac{\alpha_B^2\alpha_s^4\left(\alpha^2+{\alpha^*}^2\right)}{4} + \frac{\alpha_B^2\alpha_s^4\alpha\alpha^*}{2}\left(\frac{I_{n+1}\left(\frac{\alpha_B^2\alpha_s^2}{4}\right)}{I_n\left(\frac{\alpha_B^2\alpha_s^2}{4}\right)}\right)\right) + 3.2786\frac{C_n^2z^2}{l_0^{1/3}}.\end{aligned} \tag{2.19}$$

Finally, from (2.1), radius of curvature of Bessel-Gaussian beam will become

$$
\begin{aligned}
R(z) = & \left[\frac{(1+n)\alpha_s^2}{2} + \frac{a_B^2 \alpha_s^4}{8} \left(\frac{I_{n+1}\left(\frac{a_B^2 \alpha_s^2}{4}\right)}{I_n\left(\frac{a_B^2 \alpha_s^2}{4}\right)} - 1 \right) \right. \\
& + 2z \left(-\frac{(1+n)\alpha_s^2}{2F_0} - \frac{a_B^2 \alpha_s^4}{8F_0} \left(\frac{I_{n+1}\left(\frac{a_B^2 \alpha_s^2}{4}\right)}{I_n\left(\frac{a_B^2 \alpha_s^2}{4}\right)} - 1 \right) \right) \\
& + z^2 \left(2(1+n)\alpha_s^2 \alpha\alpha^* + \frac{a_B^2 \alpha_s^4 \left(\alpha^2 + {\alpha^*}^2\right)}{4} + \frac{a_B^2 \alpha_s^4 \alpha\alpha^*}{2} \right. \\
& \left. \left. \times \left(\frac{I_{n+1}\left(\frac{a_B^2 \alpha_s^2}{4}\right)}{I_n \frac{a_B^2 \alpha_s^2}{4}} \right) \right) + \frac{2.1857 C_n^2 z^3}{l_0^{1/3}} \right] \\
& \times \left[-\frac{(1+n)\alpha_s^2}{2F_0} - \frac{a_B^2 \alpha_s^4}{8F_0} \left(\frac{I_{n+1}\left(\frac{a_B^2 \alpha_s^2}{4}\right)}{I_n\left(\frac{a_B^2 \alpha_s^2}{4}\right)} - 1 \right) \right. \\
& + z \left(2(1+n)\alpha_s^2 \alpha\alpha^* + \frac{a_B^2 \alpha_s^4 \left(\alpha^2 + {\alpha^*}^2\right)}{4} + \frac{a_B^2 \alpha_0^4 \alpha\alpha^*}{2} \right. \\
& \left. \left. \times \left(\frac{I_{n+1}\left(\frac{a_B^2 \alpha_s^2}{4}\right)}{I_n\left(\frac{a_B^2 \alpha_s^2}{4}\right)} \right) \right) + 3.2786 \frac{C_n^2 z^2}{l_0^{1/3}} \right]^{-1}
\end{aligned}
\tag{2.20}
$$

2.2. ACCURACY OF FORMULATION

If the Bessel-Gaussian beam follows trend of the Gaussian beam, radius of curvature of the Gaussian beam can be obtained in free space by eliminating parameters, which include Bessel functions and turbulence effects in the formula of the radius of curvature for Bessel-Gaussian beam. In other words, the order of the

Bessel function of the first kind n, the width parameter a_B and the structure constant C_n^2 must be equal to zero. So, in free space, equation (2.20) will be equal to the radius of curvature of the pure Gaussian beam.

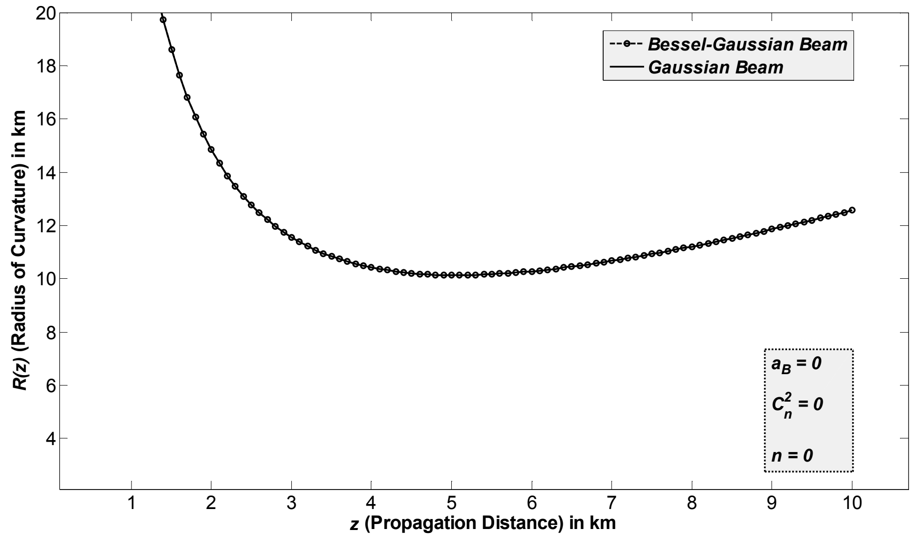

Figure 2.1 Radius of curvature of Bessel-Gaussian and Gaussian beams versus propagation distance z. For radius of curvature of Bessel-Gaussian beam, order n, the width parameter a_B and the structure constant C_n^2 is taken zero.

a_B, n and C_n^2 are eliminated in formula for the radius of curvature of the Bessel-Gaussian beam. So, as expected, the radius of curvature of the pure Gaussian beam is obtained. In Figure 2.1, this situation is shown. Radii of curvatures for the Bessel-Gaussian and Gaussian beams overlap and are equal to each other under stated conditions. Accuracy of formula (2.20) can be ensured by this way.

2.3. NUMERICAL ANALYSIS OF FORMULATION

Commonly, in free space optical systems, α_s is used as 5 cm and λ is used as $1.55\,\mu$m. Hence, in this study, when source size and wavelength are taken as constant, these parameters are used as stated above. Additionally, all plots are scaled to analyze all graphics easily. And maximum value of order for Bessel-Gaussian beam is taken as 4. Because, for the values n is bigger than 4, all plots approximate each other and overlap.

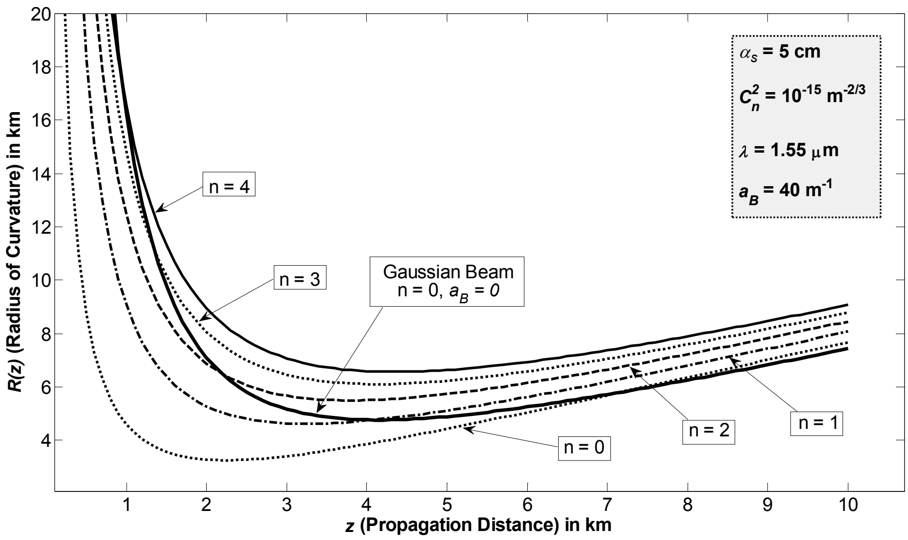

Figure 2.2 Variations of radius of curvature versus propagation distance at fixed source size, moderate turbulence level, wavelength and width parameter

In Figure 2.2, for varied orders of the Bessel function of the first kind, variations of radius of curvature of Bessel-Gaussian beam are displayed versus propagation distance at fixed source size, wavelength, width parameter and moderate turbulence level ($C_n^2 = 10^{-15}\ \mathrm{m}^{-2/3}$). Figure 2.2 indicates that radius of curvature of Bessel-Gaussian beam is infinite at first, and then the radius of curvature decreases with increasing propagation distance and reaches finite value. Finally the radius of curvature reaches its minimum value and subsequently increases with increasing propagation distance. For the bigger orders of the Bessel function of the first kind, the radius of curvature will be greater.

Beam Type	a_B in m^{-1}	n	z_R in km	$R(z)$ in km
Bessel-Gaussian Beam	40	4	4.4	6.560
		3	4.1	6.102
		2	3.8	5.492
		1	3.2	4.618
		0	2.2	3.250
Gaussian Beam	0	0	4.2	4.762

Table 2.1 In moderate turbulence level ($C_n^2 = 10^{-15}$ m$^{-2/3}$), comparison of the radii of curvatures and Rayleigh ranges of Bessel-Gaussian beam and Gaussian beam

In Table 2.1, it is obviously seen that Rayleigh ranges of Bessel-Gaussian beam increase with increasing order under condition of moderate turbulence level. When Bessel-Gaussian and Gaussian beams are compared with each other, it is seen that Bessel-Gaussian beam propagates farther than Gaussian beam before spreading out for order $n \geq 4$.

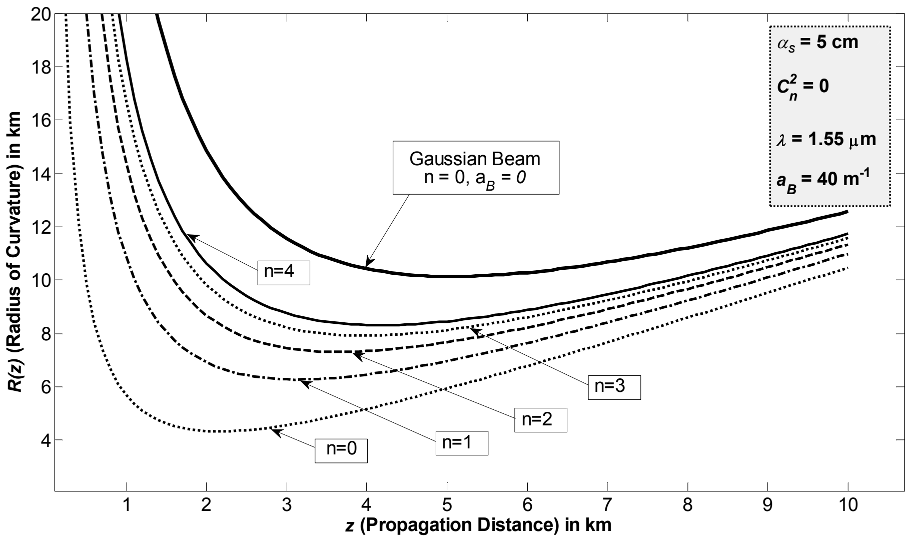

Figure 2.3 Variations of radius of curvature versus propagation distance under free space conditions at fixed source size, wavelength and width parameter

In Figure 2.3, for varied orders of the Bessel function of the first kind, variations of radius of curvature of Bessel-Gaussian beam are displayed versus propagation distance at fixed source size, wavelength, width parameter and under free space condition ($C_n^2 = 0$). Figure 2.3 indicates that there is no turbulence where radius of curvature is longer and for the higher orders of the Bessel function of the first kind, the radius of curvature will be greater. Likewise, for lower orders of the Bessel function of the first kind, the radius of curvature will be smaller.

Beam Type	a_B in m^{-1}	n	z_R in km	$R(z)$ in km
Bessel-Gaussian Beam	40	4	4.2	8.308
		3	4	7.913
		2	3.7	7.305
		1	3.1	6.270
		0	2.2	4.329
Gaussian Beam	0	0	5.1	1.013

Table 2.2 In free space ($C_n^2 = 0$), comparison of the radii of curvatures and Rayleigh ranges of Bessel-Gaussian beam and Gaussian beam

In Table 2.3, under condition of free space, Gaussian beam propagates farther than Bessel-Gaussian beam. But, in practice, there is always atmospheric turbulence.

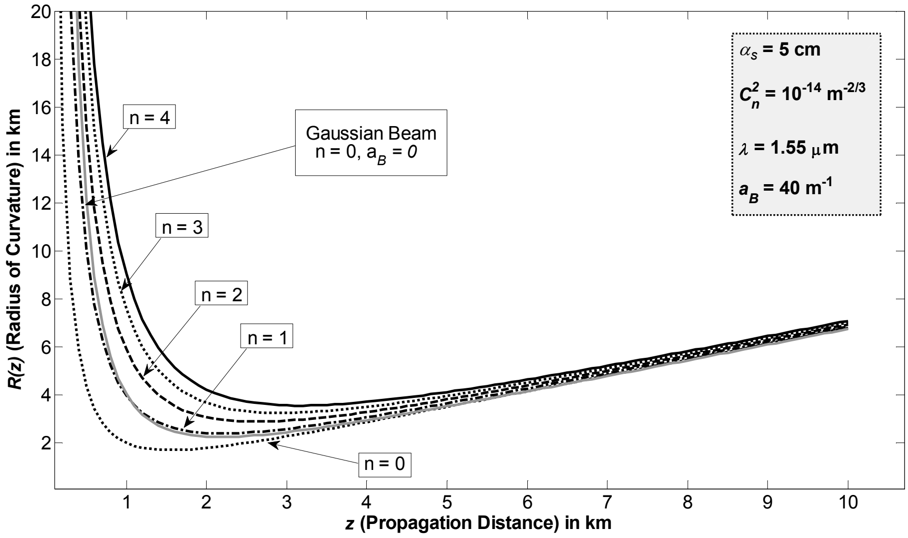

Figure 2.4 Variations of radius of curvature versus propagation at fixed source size, high turbulence level, wavelength and width parameter

In Figure 2.4, for varied orders of the Bessel function of the first kind, variations of radius of curvature of Bessel-Gaussian beam are displayed versus propagation distance at fixed source size, wavelength, width parameter and high turbulence level ($C_n^2 = 10^{-14}\ \mathrm{m}^{-2/3}$). Figure 2.4 indicates that high turbulence levels suppress radii of curvatures for all orders.

For Figures 2.2, 2.3 and 2.4, it is seen that radii of curvatures of Bessel-Gaussian beam show the same behavior. For all orders of Bessel-Gaussian beam, radii of curvatures decrease with growing turbulence levels. It is also clear that Bessel-Gaussian beam follows the trend of Gaussian beam.

Beam Type	a_B in m^{-1}	n	z_R in km	$R(z)$ in km
Bessel-Gaussian Beam	40	4	3.2	3.558
		3	2.9	3.255
		2	2.6	2.885
		1	2.2	2.399
		0	1.5	1.706
Gaussian Beam	0	0	2.2	2.250

Table 2.3 In high turbulence level ($C_n^2 = 10^{-14}\ \mathrm{m}^{-2/3}$), comparison of the radii of curvatures and Rayleigh ranges of Bessel-Gaussian beam and Gaussian beam

Under condition of high turbulence level, Table 2.2 shows that Bessel-Gaussian beam propagates farther than Gaussian beam before spreading out for order $n \geq 1$. Rayleigh range and radius of curvature of Bessel-Gaussian beam deacrese with increasing turbulence levels.

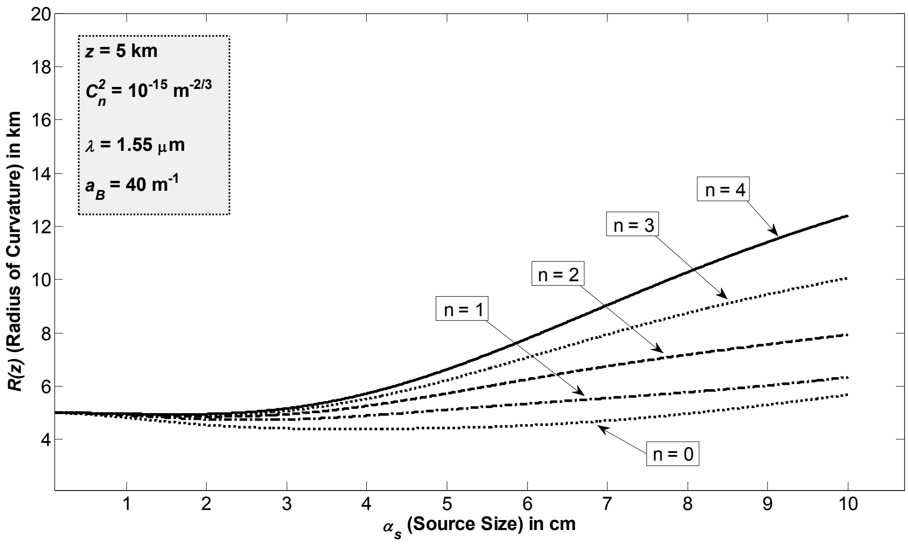

Figure 2.5 Variations of radius of curvature versus source size at fixed propagation distance, moderate turbulence level, wavelength and width parameter

In Figure 2.5, for varied orders of the Bessel function of the first kind, variations of radius of curvature of Bessel-Gaussian beam are displayed versus propagation distance at fixed source size, wavelength, width parameter and moderate turbulence level ($C_n^2 = 10^{-15}\ \mathrm{m}^{-2/3}$). Figure 2.5 indicates that at smaller source sizes, radius of curvature is around propagation distance and at bigger source sizes, radius of curvature increases sharply with growing orders of the Bessel function of the first kind.

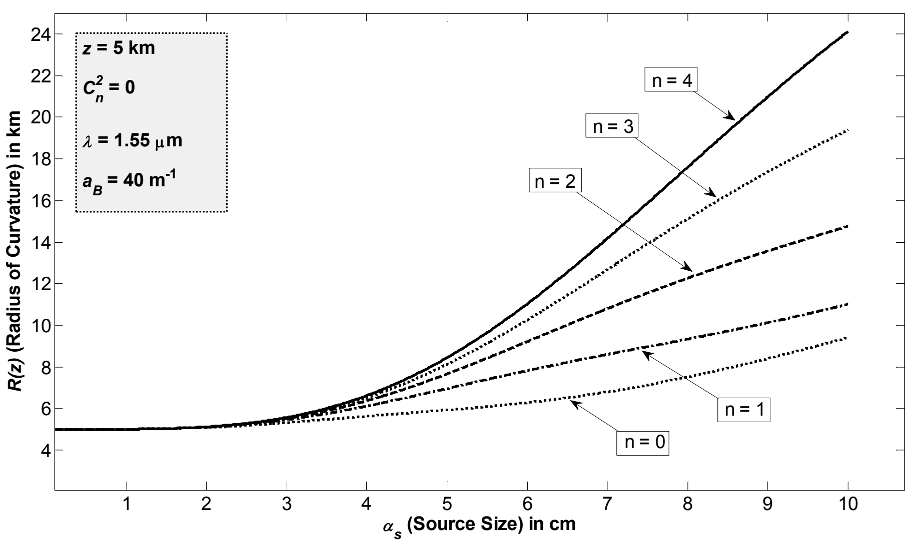

Figure 2.6 Variations of radius of curvature versus source size under free space conditions at fixed propagation distance, wavelength and width parameter

In Figure 2.6, for varied orders of the Bessel function of the first kind, variations of radius of curvature of Bessel-Gaussian beam are displayed versus propagation distance at fixed source size, wavelength, width parameter and under free space condition ($C_n^2 = 0$). Figure 2.6 indicates that at smaller source sizes, radius of curvature is around propagation distance but because of there is no turbulence, at bigger source sizes, radius of curvature rises more sharply with growing orders of the Bessel function of the first kind.

The comparison of Figures 2.5 and 2.6 shows that again, for all orders of Bessel-Gaussian beam, radii of curvatures are decreased by growing turbulence levels.

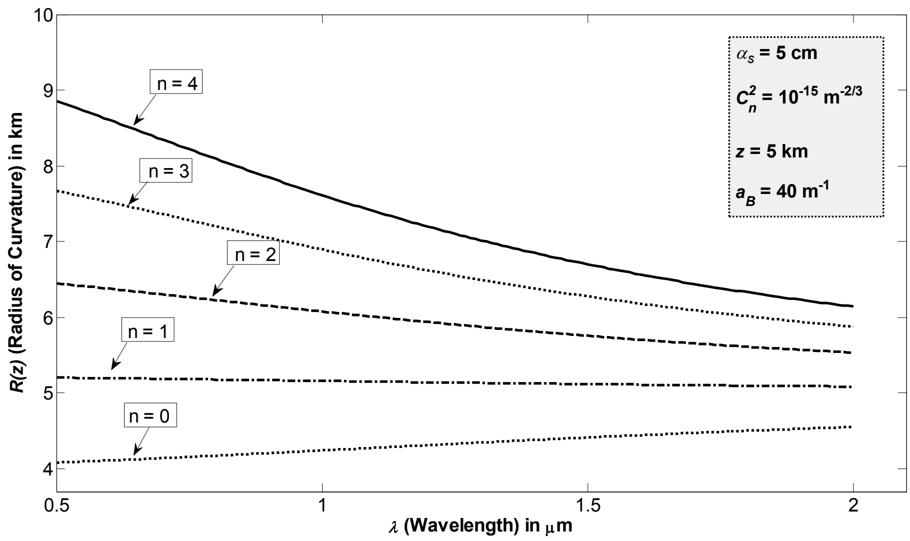

Figure 2.7 Variations of radius of curvature versus wavelength at fixed propagation distance, source size, moderate turbulence level and width parameter

In Figure 2.7, for varied orders of the Bessel function of the first kind, variations of radius of curvature of Bessel-Gaussian beam are displayed versus wavelength at fixed source size, propagation distance, width parameter and moderate turbulence level ($C_n^2 = 10^{-15}\ \mathrm{m}^{-2/3}$). Figure 2.7 indicates that radius of curvature decreases with increasing wavelength except the condition of lowest order of Bessel-Gaussian beam.

CONCLUSION

With the help of previous studies, the radius of curvature of the Bessel-Gaussian beam has been developed and its accuracy has been verified. Effects of atmospheric turbulence on the radius of curvature of Bessel-Gaussian beam are analyzed. The radius of curvature of the Bessel-Gaussian beam versus the propagation distance, source size and wavelength graphs show that the radii of curvatures of the Bessel-Gaussian beam act as the Gaussian beam under different conditions. In all plotted figures, radii of curvatures decrease with growing turbulence effect. Especially, in the radius of curvature of Bessel-Gaussian beam versus the propagation distance graph, radii of curvatures are infinite at the source, and then decrease until they reach a minimum value. After they reach their minimum, the radii of curvatures approximate to infinity for very large propagation distances. This minimum value is determined always as their Rayleigh range z_R.

As it is known, in the optical systems, a beam can propagate to distance of the Rayleigh range before it spreads out in free space [13]. Also, in the optical systems, it is important to transmit a signal to the farthest point with minimum loss. If these two cases are taken into account, the beam, which has the highest Rayleigh range, can be selected. From tables, according to distance, where data is desired to be sent, beam type or order can be selected. It must be taken into account that increasing radius of curvature with increasing propagation distance causes the beam width to expand.

In addition, the radius of curvature of Bessel-Gaussian beam increases with increasing source size and increasing order (n) of the Bessel function at a fixed propagation distance. Also, when wavelength is increased, the radius of curvature stays same for lowest order of Bessel-Gaussian beam and the radius of curvature decreases for other orders.

REFERENCES

[1] Andrew W., Rebeiro T., Rodney T., (2006) Free Space Optical Laser Communication Link, Jasa, 50-52. Vol. 1.

[2] Heinz Willebrand, Baksheesh S. Ghuman, (2001) Free Space Optics: Enabling Optical Connectivity in Today's Networks, (First Ed.), SAMS, Indiana USA

[3] Özsoy S., (2001) Fiber Optik, (2th Ed.), Birsen Yayınevi, İstanbul

[4] Eyyuboğlu, H.T., Ji, X.L., (2010) An Analysis on Radius of Curvature Aspects of Hyperbolic and Sinusoidal Gaussian Beams, Springer-Verlag, 1-2. Vol. 101.

[5] Eyyuboğlu, H.T., Baykal, Y.K., Ji, X.L., (2010) Radius of Curvature Variations for Annular, Dark Hollow and Flat Topped Beam in Turbulence, Springer-Verlag, 4. Vol. 99.

[6] Amnon Y., (1988) Quantum Electronics, (3th Ed.), Wiley, USA

[7] Saleh, B.E.A., Teich, M.C., (2007), Fundamental of Photonics, (2nd Ed.), Wiley.

[8] Riley, K.F., Hobson, M.P., Bence, S. J., (2006) Mathematical Methods for Physics and Engineering, (3th Ed.), Cambridge University Press

[9] Eyyuboğlu, H.T., Sermutlu, E., Baykal, Y., Cai, Y., Korotkova, O., (2008) Intensity Fluctuations in J-Bessel-Gaussian Beams of All Orders Propagating in Turbulent Atmosphere, Springer- Verlag, 2-3. Vol. 1.

[10] Gradshteyn, I.S., Ryzhik I.M. (2007), Table of Integrals, Series and Products (7th Ed.), Elsevier.

[11] Andrews, L.C., Philips, R.L., (2005), Laser Beam Propagation through Random Media, (2th Ed.), Spie Press, Bellingham, Washington USA.

[12] Eyyuboğlu, H.T., (2007) Propagation of Higher Order Bessel-Gaussian Beams in Turbulence, Springer-Verlag, 2. Vol. 88.

[13] Quimby, R.S., (2006) Photonics and Lasers: An Introduction, (First Ed.)

[14] Siegman, A.E., (1986), Lasers, University Science Books, Mill Valley, CA.

CURRICULUM VITAE

PERSONAL INFORMATION

Surname, Name: AKKOYUN, Sıdıka Türkan
Nationality: Turkish (TC)
Date and Place of Birth: 10 February 1984, AYDIN/Söke
Marital Status: Single
Phone: 0544 404 84 19
email: sidikaakkoyun@gmail.com

EDUCATION

Degree	Institution	Year of Graduation
BS	Çanakkale 18 Mart Univ. Physics	2007
High School	Söke High School	2002

WORK EXPERIENCE

Year	Place	Enrollment
2008	Türksat	Intern

FOREIGN LANGUAGES

Advanced English

HOBBIES

Travel, music, playing guitar, cinema, reading book